Klym et al. Nanoscale Research Letters (2016) 11:133
DOI 10.1186/s11671-016-1352-6

Nanoscale Research Letters
a SpringerOpen Journal

NANO EXPRESS Open Access

Water-Vapor Sorption Processes in Nanoporous MgO-Al_2O_3 Ceramics: the PAL Spectroscopy Study

Halyna Klym[1*], Adam Ingram[2], Oleh Shpotyuk[3,4], Ivan Hadzaman[5] and Viacheslav Solntsev[6]

Abstract

The water-vapor sorption processes in nanoporous MgO-Al_2O_3 ceramics are studied with positron annihilation lifetime (PAL) spectroscopy employing positron trapping and positronium (Ps)-decaying modes. It is demonstrated that the longest-lived components in the four-term reconstructed PAL spectra with characteristic lifetimes near 2 and 60–70 ns can be, respectively, attributed to ortho-positronium (o-Ps) traps in nanopores with 0.3- and 1.5–1.8-nm radii. The first o-Ps decaying process includes "pick-off" annihilation in the "bubbles" of liquid water, while the second is based on o-Ps interaction with physisorbed water molecules at the walls of the pores. In addition, the water vapor modifies structural defects located at the grain boundaries in a vicinity of pores, this process being accompanied by void fragmentation during water adsorption and agglomeration during water desorption after drying.

Keywords: Positron annihilation, Trapping, Positronium, Ceramics, Nanopores, Water sorption

Background

Functional $MgAl_2O_4$ ceramics (MgO-Al_2O_3) with a spinel structure are known as excellent porous materials for humidity sensors [1–3]. These ceramics are thermally and chemically stable in comparison with other types of porous media possessing fast response to humidity changes [4]. An actual challenge is related to porous materials with a controllable microstructure, large specific surface area, high open porosity, optimal pore size, and distribution of free-volume entities [5, 6].

The effect of initial surface area of powdered binary oxide ingredients (MgO and Al_2O_3) on the structure of MgO-Al_2O_3 ceramics sintered at 1100–1400 °C was studied extensively in [7–10]. It was shown that the formation of this spinel-structured ceramics is substantially intensified with increase in sintering temperature and duration. In addition, the sintering temperature possessed an essential effect on the pore structure and exploitation properties of $MgAl_2O_4$ ceramics [7].

Traditionally, the microstructures of porous ceramics are studied using X-ray (electron, neutron) diffraction, electron microscopy, and different direct porosimetric methods [11–13]. However, the techniques of mercury and/or nitrogen intrusion porosimetry provide reliable information on open pores with radii over 2 nm [14], whereas physical processes in such ceramics depend on not only large open pores but closed nanopores too [15].

To gain knowledge about such fine free-volume entities and their effect on $MgAl_2O_4$ ceramics, it is reasonable to use the method of positron annihilation lifetime (PAL) spectroscopy, which is an alternative probe of structural characterization allowing the study of both closed and open pores at a nanoscale [16]. Two channels of positron annihilation were shown to be important in case of ceramics: positron trapping and ortho-positronium (o-Ps) decaying [17–19]. The latter process ("pick-off" annihilation) resulting from positronium (Ps) interaction with electron from environment (including annihilation in liquid water) is ended by emission of two γ-quanta [17]. In general, these two channels of positron annihilation are independent. However, if trapping sites will appear in a vicinity of grain boundaries neighboring with free-volume pores, these positron-Ps traps become mutually interconnected resulting in a significant complication of PAL data.

In this work, we use the PAL method developed in positron trapping and o-Ps-decaying modes to characterize

* Correspondence: klymha@yahoo.com
[1]Lviv Polytechnic National University, 12 Bandera str., 79013 Lviv, Ukraine
Full list of author information is available at the end of the article

MgO-Al_2O_3 ceramics sintered at 1100–1400 °C in different stages of water-vapor sorption and drying treatment.

Methods

The MgO-Al_2O_3 ceramics were sintered at maximal temperatures (T_s) of 1100, 1200, 1300, and 1400 °C for 2 h, as it was described elsewhere [7, 9, 20, 21]. In respect to X-ray diffraction measurements [7], the ceramics prepared at lower T_s = 1100–1200 °C are composed of the main spinel phase and a large amount of additional MgO and Al_2O_3 phases (up to 12 %), while the ceramics sintered at high T_s of 1300 and 1400 °C contain additionally only the MgO phase in the amount of 3.5 and 1.5 %, respectively.

The PAL measurements were performed with the ORTEC instrument (using ^{22}Na source placed between two identical sandwiched samples) [7, 22] at 22 °C and relative humidity RH = 35 % after drying, 7 days of water exposure (water vapor in a desiccator at RH = 100 %), and further final drying in a vacuum at 120 °C for 4 h. Each PAL spectrum was collected within a 6.15-ps channel width to analyze short and intermediate PAL components. To obtain data on longest-lived PAL components, the same ceramics were studied within a channel width of 61.5 ps [15]. The collected spectra were analyzed with LT software [23]. In previous works [8–10], we used three-component fitting procedures under normal statistical treatment of PAL spectra accumulated near one million of elementary positron annihilation events. At high-statistical measurements (more than ten million counts), the best results were obtained with a four-term decomposition procedure. Such approach allows us to study nanopores of different sizes, responsible for o-Ps decaying. Each PAL spectrum was processed multiply owing to slight changes in the number of final channels, annihilation background, and time shift of the 0th channel. In such a manner, we obtained fitting parameters (positron lifetimes τ_1, τ_2, τ_3, τ_4 and corresponding unity-normalized intensities I_1, I_2, I_3, I_4), which correspond to annihilation of positrons in the samples of interest within a quite reliable error bar.

Results and Discussion

Typical PAL spectra of MgO-Al_2O_3 ceramics sintered at 1400 °C detected within 6.15- and 61.5-ps channel widths are shown in Fig. 1. Four discrete exponentially decaying components were reconstructed from these spectra using the known LT program [23]. Fitting curves for all components in the region of PAL spectra's peaks are depicted in more detail in the inserts of Fig. 1.

As it was shown earlier [7–10], the positron annihilation in humidity-sensitive MgO-Al_2O_3 ceramics is revealed through two different channels related to "free" positron trapping (the intermediate component with lifetime τ_2) and o-Ps decaying (two long-lived components with τ_3 and τ_4 lifetimes). The first component with parameters τ_1 and I_1 reflects mainly microstructure specificity of spinel ceramics with character octahedral and tetrahedral vacant cation sites along with input from annihilation of para-Ps atoms. The intermediate lifetime τ_2 is related to the size of free-volume defects near grain boundaries, and I_2 intensity reflects their amount [10]. The third and fourth components (τ_3, I_3) and (τ_4, I_4), respectively, originate from annihilation of o-Ps atoms in intrinsic nanopores of MgO-Al_2O_3 ceramics [7, 24].

Fitting parameters obtained within the four-component treatment of the reconstructed PAL spectra of initially dried, water-vapored, and finally dried MgO-Al_2O_3 ceramics sintered at 1100–1400 °C are gathered in Table 1. It is established that τ_1 lifetime in the dried ceramics decreases with T_s, while I_1 intensity increases in respect to the amount of main spinel phase like in [7, 10]. Positrons are trapped more strongly in ceramics prepared at lower T_s, as reflected in the values of the second component of the reconstructed PAL spectra. As it follows from Table 1, the numerical values of this component (τ_2 and I_2) decrease with T_s (so positron-trapping parameters calculated within a two-state trapping model [16] will be also changed).

As it follows from Table 2, the calculated values of positron trapping modes in MgO-Al_2O_3 ceramics (average positron lifetime $\tau_{av.}$, bulk positron lifetimes in defect-free samples τ_b, and positron trapping rates in defects κ_d) are decreased with sintering temperature T_s. These parameters are in good agreement with the amount of additional MgO and Al_2O_3 phases in the ceramics [7].

At the same time, the principal water-vapor sorption processes in the studied MgO-Al_2O_3 ceramics sintered at 1100–1400 °C occur to be mostly determined by o-Ps-related components in the PAL spectra reconstructed through the four-term fitting procedure (Fig. 1). Some details of PAL spectra of the ceramics sintered at different T_s are shown in the region of the main peak and long fluent decaying of coincidence counts at a certain time in Fig. 2. As it was shown earlier [7, 15], the corresponding long-lived lifetimes τ_3 and τ_4 reflect sizes of nanopores, and their intensities I_3 and I_4 are directly related to the number of these nanopores [7, 15].

So, in the initially dried MgO-Al_2O_3 ceramics sintered at 1100–1400 °C, the lifetime τ_3 increases with T_s, while intensity I_3 decreases (Table 1). These changes are due to the increase in the size of small nanopores with radius R_3, and their reduction is caused by increasing contact between grains. The lifetime τ_4 and intensity I_4 naturally decrease with T_s, indicating reduction in size and number of nanopores with radius R_4. The radii R_3 and R_4 of spherical nanopores (given in Table 2) were calculated using o-Ps-related τ_3 and τ_4 lifetimes in the known Tao-Eldrup model [25, 26]:

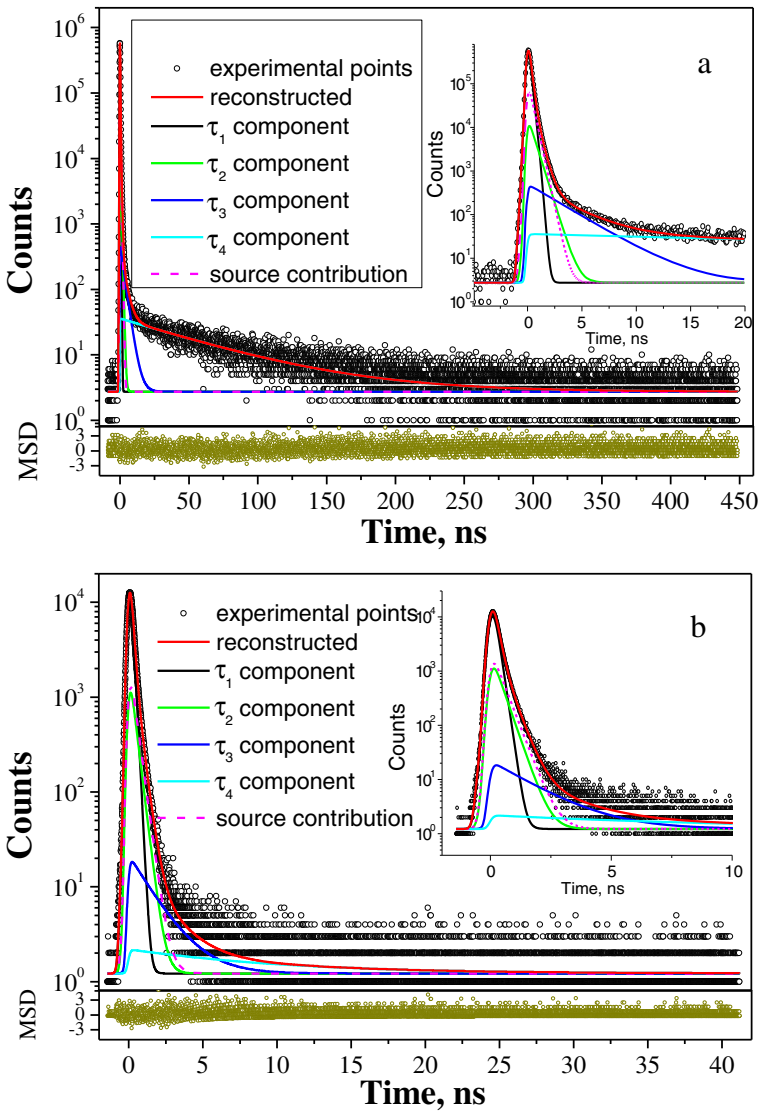

Fig. 1 PAL spectra of MgO-Al_2O_3 ceramics sintered at 1400 °C registered at channel widths of 61.5 ps (**a**) and 6.15 ps (**b**), reconstructed from four-term fitting at the general background of source contribution (bottom *inset* shows statistical scatter of variance)

$$\tau_{\text{o - Ps}} = \left[2\left(1-\frac{R}{R+\Delta R}+\frac{1}{2\pi}\sin\left(\frac{2\pi R}{R+\Delta R}\right)\right)+0.007\right]^{-1}, \quad (1)$$

where ΔR is an empirically derived parameter ($\Delta R \approx 0.1656$ nm for polymers [18]), which describes effective thickness of the electron layer responsible for the "pick-off" annihilation of o-Ps in a hole.

It is shown that the radius of nanopores R_3 increases from 0.309 to 0.331 nm and R_4 remains nearly at the same level (~1.8 nm) in the initially dried ceramics sintered at 1100–1400 °C (Fig. 3). In addition, free-volume fraction f_v (Table 2) was evaluated using o-Ps-related intensities $I_{\text{o-Ps}}$ corresponding to the third I_3 and fourth I_4 components of the PAL spectra:

$$f_v = C \cdot V_f \cdot I_{\text{o-Ps}}, \quad (2)$$

where $V_f = 4/3 \cdot \pi \cdot R_{\text{o-Ps}}^3$ is the free volume of a nanopore calculated using o-Ps-related components in spherical approximation and C is an empirical parameter equal to 0.0018 [18].

Preferential decreasing of the lifetime τ_2 in water-vapored MgO-Al_2O_3 ceramics and increasing of their intensity I_2 demonstrates intensification of positron trapping in defects near grain boundaries filled with water. After final drying, the intensities I_2 practically completely return to the initial values (character for initially dried samples), whereas τ_2 lifetimes are larger in ceramics sintered at 1300 and 1400 °C. Thus, the water adsorption processes in MgO-Al_2O_3 ceramics are accompanied by fragmentation of positron

Table 1 Fitting parameters describing PAL spectra of MgO-Al_2O_3 ceramics sintered at different T_s temperatures reconstructed from a four-term decomposition procedure

Sample	τ_1 (±0.002), ns	I_1 (±1), %	τ_2 (±0.005), ns	I_2 (±1), %	τ_3 (±0.002), ns	I_3 (±0.2), %	τ_4 (±0.02), ns	I_4 (±0.1), %
T_s = 1100 °C								
Initial drying	0.169	68	0.462	28	2.240	1.7	70.14	2.5
Water vapor	0.170	66	0.483	28	1.820	4.4	53.05	0.9
Final drying	0.172	68	0.459	29	2.215	2.1	68.29	1.9
T_s = 1200 °C								
Initial drying	0.164	73	0.443	24	2.347	1.1	70.51	2.0
Water vapor	0.160	64	0.426	31	2.047	3.8	58.67	0.4
Final drying	0.163	72	0.429	23	2.290	3.1	68.87	1.7
T_s = 1300 °C								
Initial drying	0.155	82	0.414	16	2.426	0.8	68.74	1.4
Water vapor	0.161	76	0.400	21	2.619	1.8	58.33	0.7
Final drying	0.156	82	0.421	15	2.448	0.7	68.17	1.4
T_s = 1400 °C								
Initial drying	0.152	88	0.388	11	2.504	0.7	62.32	0.8
Water vapor	0.160	77	0.409	20	2.562	2.2	57.35	0.6
Final drying	0.154	89	0.402	10	2.539	0.7	61.85	0.8

trapping sites near grain boundaries, and, respectively, the water desorption processes are accompanied by agglomeration of free-volume voids.

Water-vapor sorption processes in the studied ceramics result in essential evolution of the third and fourth o-Ps-related components. The intensity I_3 increases in all initially dried samples after water-vapor exposure, thus confirming o-Ps annihilation in water-filled nanopores through a "bubble" mechanism (with corresponding o-Ps lifetime close to 1.8 ns) [27–29]. At the same time, the lifetime τ_3 decreases in more defective ceramics sintered at 1100 and 1200 °C but increases in more perfect ceramics sintered at 1300 and 1400 °C. After final drying, the intensity I_3 for ceramics sintered at 1100 and 1200 °C is not returned to initial values.

Table 2 Positron trapping modes and free-volume nanopore parameters related to o-Ps decaying determined from four-term decomposed PAL spectra of MgO-Al_2O_3 ceramics sintered at different T_s temperatures

Sample	Positron trapping modes			Free-volume parameters			
	τ_{av}, ns	τ_b, ns	κ_d, ns^{-1}	R_3, nm	$\sim f_3$, %	R_4, nm	$\sim f_4$, %
T_s = 1100 °C							
Initial drying	0.254	0.21	1.10	0.309	0.38	1.844	11.75
Water vapor	0.263	0.21	1.15	0.271	0.66	1.539	2.43
Final drying	0.257	0.21	1.08	0.307	0.46	1.810	8.36
T_s = 1200 °C							
Initial drying	0.232	0.19	0.94	0.319	0.26	1.852	9.62
Water vapor	0.252	0.21	1.19	0.293	0.72	1.636	1.16
Final drying	0.229	0.19	0.93	0.296	0.61	1.821	7.77
T_s = 1300 °C							
Initial drying	0.197	0.17	0.66	0.325	0.20	1.818	6.18
Water vapor	0.213	0.19	0.80	0.340	0.52	1.630	2.40
Final drying	0.198	0.17	0.63	0.327	0.20	1.807	6.06
T_s = 1400 °C							
Initial drying	0.178	0.16	0.44	0.331	0.19	1.701	3.07
Water vapor	0.211	0.18	0.78	0.335	0.63	1.613	1.74
Final drying	0.179	0.16	0.40	0.334	0.19	1.692	3.02

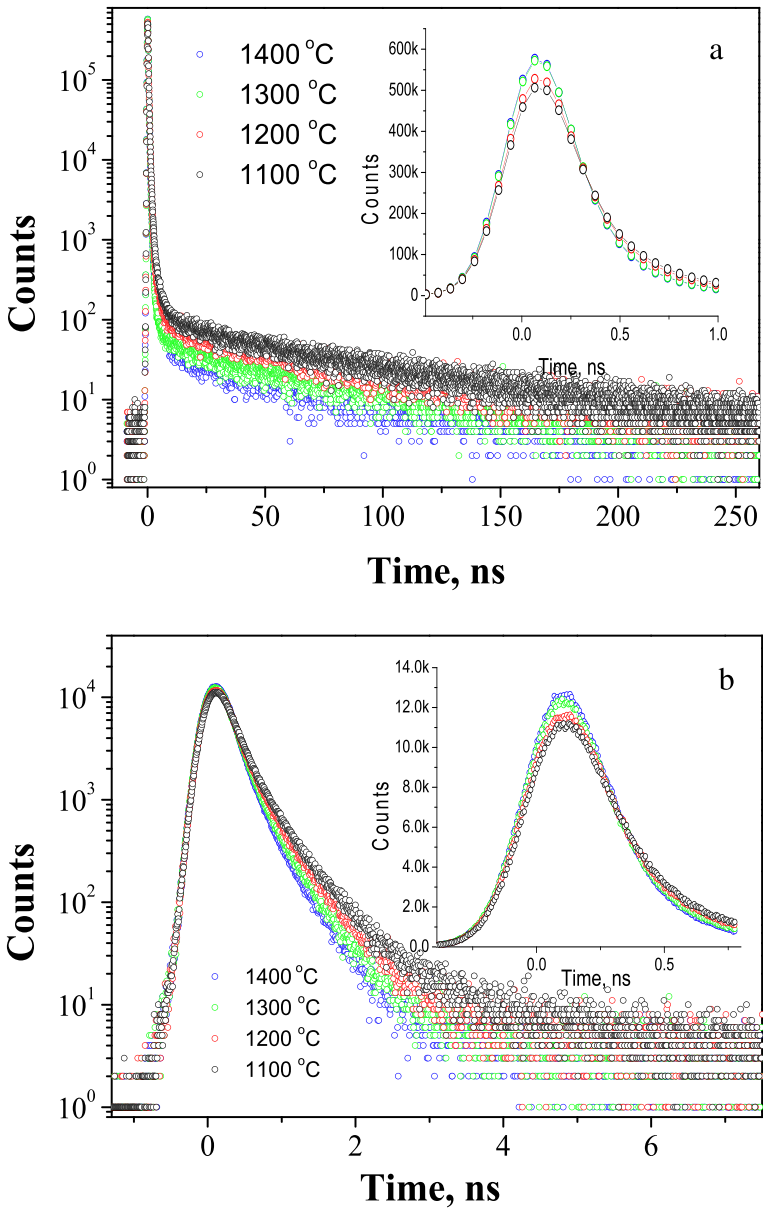

Fig. 2 PAL spectra of MgO-Al_2O_3 ceramics sintered at 1100–1400 °C registered under channel widths of 61.5 ps (**a**) and 6.15 ps (**b**)

This confirms the remainder of sorbed water in the nanopores with size near 0.3 nm and slight desorption ability of these MgO-Al_2O_3 ceramics samples (Fig. 3). In MgO-Al_2O_3 ceramics sintered at 1300 and 1400 °C, the intensity of the third component returns to initial value, confirming high efficiency of water adsorption-desorption processes.

Another mechanism of water-vapor sorption processes similar to one reported in [30] is realized in the studied MgO-Al_2O_3 ceramics through the fourth component of the PAL spectra. Unlike the third component, the intensity I_4 decreases in water-vapor exposure ceramics samples. Since this intensity does not drop to zero being within 0.4–0.9 % domain, it should be assumed that there exists a fraction of closed nanopores where o-Ps are trapped [15]. After final drying (in a vacuum at 120 °C for 4 h) of the ceramics samples previously exposed to water vapor, the initial pore size tends to be restored (Table 2 and Fig. 3). However, it does not recover entirely, suggesting that some fraction of water molecules remain adsorbed. The intensity I_4 does not return to initial value in ceramics sintered at 1100 and 1200 °C with poorly developed open porosity (Table 1). Most probably, physically adsorbed water is not fully eliminated at 120 °C in these ceramics samples. The decreased τ_4 value for ceramics dried after water-vapor exposure can be connected with formation of thin layers of water molecules covering the walls of pores with radii of 1.5–1.8 nm,

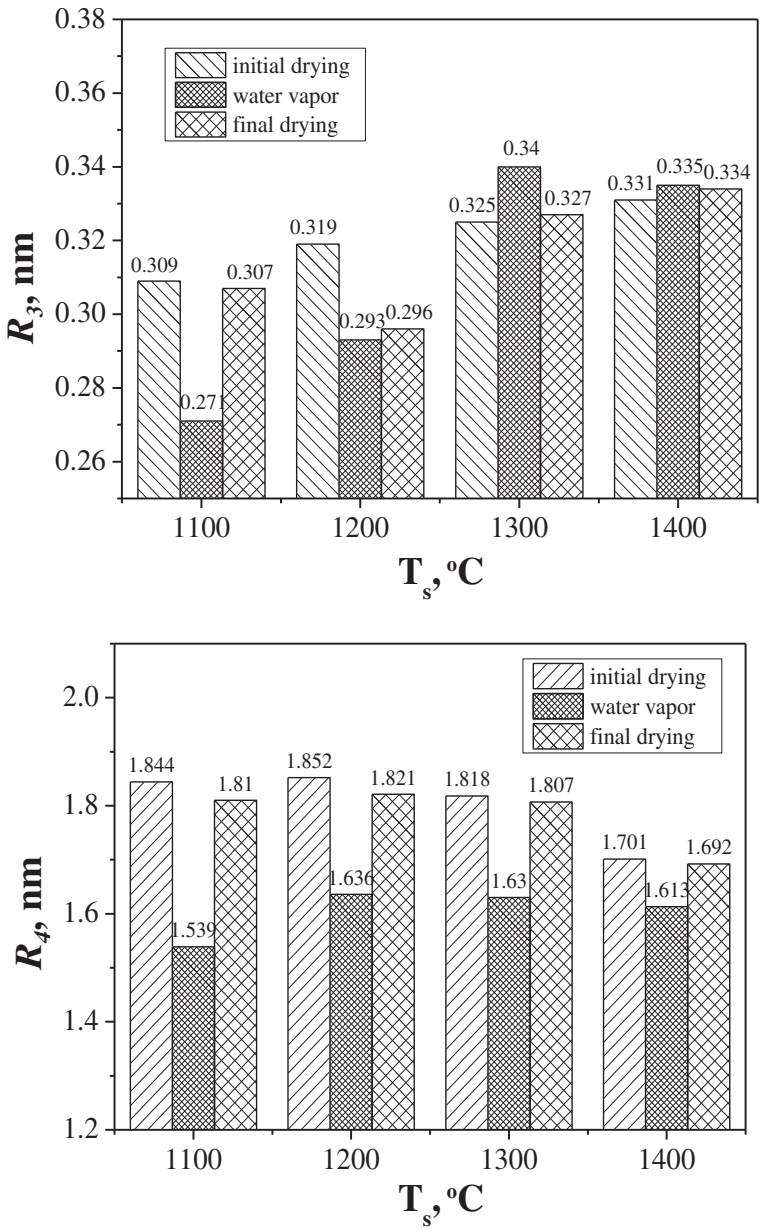

Fig. 3 Nanopore radii R_3 and R_4 in MgO-Al_2O_3 ceramics sintered at 1100–1400 °C changed in water adsorption-desorption cycles

which are not completely removed after vacuum annealing at 120 °C for 4 h.

Conclusions

The method of PAL spectroscopy in high-measurement statistics is employed to study water-vapor sorption processes in MgO-Al_2O_3 ceramics sintered at 1100–1400 °C temperatures for 2 h. It is shown that positrons are trapped more strongly in the ceramics obtained at lower T_s, which was reflected in the second component of the four-term decomposed PAL spectra. The third and fourth longest-lived components in these spectra are due to annihilation of o-Ps atoms in the nanopores, the corresponding radii being calculated from τ_3 and τ_4 lifetimes using the known Tao-Eldrup model. The final drying in a vacuum at 120 °C for ceramics previously exposed to water vapor does not restore initial pore size, confirming sensitivity of PAL method to the amount of water molecules adsorbed in the nanopores. The Ps annihilation in nanopores with adsorbed water vapor is shown to occur via two mechanisms: (1) o-Ps decaying in nanopores with radius of 0.3 nm including "pick-off"

annihilation in the "bubbles" of liquid water and (2) o-Ps trapping in free volume of nanopores (1.5–1.8 nm) with physisorbed water molecules at the pore walls. The water vapor modifies defects in ceramics located near grain boundaries, this process accompanied by void fragmentation at water adsorption with further void agglomeration at water desorption after drying.

Competing Interests
The authors declare that they have no competing interests.

Authors' Contributions
HK performed the experiments to study the nanopore transformation caused by the water-vapor sorption process in the MgO-Al_2O_3 ceramics and drafted, wrote, and arranged the article. AI participated in the PAL measurements and treatment of spectra. OSh supervised the work and finalized the manuscript. IH sintered the ceramics samples. VS participated in the treatment of the PAL data. All authors read and approved the final manuscript.

Acknowledgements
H. Klym thanks the Lviv Polytechnic University under Doctoral Program and support via Project DB/KIBER (No 0115U000446).

Author details
[1]Lviv Polytechnic National University, 12 Bandera str., 79013 Lviv, Ukraine. [2]Physics Faculty of Opole University of Technology, 75 Ozimska str., 45370 Opole, Poland. [3]Vlokh Institute of Physical Optics, 23 Dragoanova str., Lviv 79005, Ukraine. [4]Institute of Physics of Jan Dlugosz University, 13/15 al. Armii Krajowej, Czestochowa 42201, Poland. [5]Drohobych State Pedagogical University, I. Franko str., 24, Drohobych 82100, Ukraine. [6]V.E. Lashkaryov Institute of Semiconductor Physics of National Academy of Sciences of Ukraine, 41, Prospekt Nauki, 03680 Kiev, Ukraine.

Received: 30 November 2015 Accepted: 1 March 2016
Published online: 09 March 2016

References
1. Kulwicki BM (1991) Humidity sensors. J Am Ceram Soc 74(4):697–708
2. Gusmano G, Montesperelli G, Traversa E, Bearzotti A, Petrocco G, D'amico A, Di Natale C (1992) Magnesium aluminium spinel as humidity sensor. Sensors Actuators B Chem 7:460–463
3. Traversa E (1995) Ceramic sensors for humidity detection: the state-of-the-art and future developments. Sensors Actuators B Chem 23(2):135–156
4. Gusmano G, Montesperelli G, Traversa E, Mattogno G (1993) Microstructure and electrical properties of $MgAl_2O_4$ thin films for humidity sensing. J Am Ceram Soc 76(3):743–750
5. Kashi MA, Ramazani A, Abbasian H, Khayyatian A (2012) Capacitive humidity sensors based on large diameter porous alumina prepared by high current anodization. Sensors Actuators A 174:69–74
6. Armatas GS, Salmas CE, Louloudi MG, Androutsopoulos P, Pomonis PJ (2003) Relationships among pore size, connectivity, dimensionality of capillary condensation, and pore structure tortuosity of functionalized mesoporous silica. Langmuir 19:3128–3136
7. Klym H, Ingram A, Hadzaman I, Shpotyuk O (2014) Evolution of porous structure and free-volume entities in magnesium aluminate spinel ceramics. Ceram Int 40(6):8561–8567
8. Klym H, Ingram A, Shpotyuk O, Filipecki J, Hadzaman I (2011) Structural studies of spinel manganite ceramics with positron annihilation lifetime spectroscopy. J Phys Conf Ser 289(1):012010
9. Filipecki J, Ingram A, Klym H, Shpotyuk O, Vakiv M (2007) Water-sensitive positron trapping modes in nanoporous magnesium aluminate ceramics. J Phys Conf Ser 79(1):012015
10. Klym H, Ingram A (2007) Unified model of multichannel positron annihilation in nanoporous magnesium aluminate ceramics. J Phys Conf Ser 79(1):012014
11. Karbovnyk I, Lesivtsiv V, Bolesta I, Velgosh S, Rovetsky I, Pankratov V, Balasubramanian C, Popov AI (2013) BiI_3 nanoclusters in melt-grown CdI_2 crystals studied by optical absorption spectroscopy. Phys B Condens Matter 413:12–14
12. Karbovnyk I, Bolesta I, Rovetski I, Velgosh S, Klym H (2014) Studies of CdI_2–Bi_3 microstructures with optical methods, atomic force microscopy and positron annihilation spectroscopy. Mater Sci Pol 32(3):391–395
13. Bondarchuk A, Shpotyuk O, Glot A, Klym H (2012) Current saturation in In_2O_3-SrO ceramics: a role of oxidizing atmosphere. Rev Mex Fis 58:313–316
14. Hajnos M, Lipiec J, Świeboda R, Sokołowska Z, Witkowska-Walczak B (2006) Complete characterization of pore size distribution of tilled and orchard soil using water retention curve, mercury porosimetry, nitrogen adsorption, and water desorption methods. Geoderma 135:307–314
15. Golovchak R, Wang S, Jain H, Ingram A (2012) Positron annihilation lifetime spectroscopy of nano/macroporous bioactive glasses. J Mater Res 27(19):2561–2567
16. Kobayashi Y, Ito K, Oka T, Hirata K (2007) Positronium chemistry in porous materials. Radiat Phys Chem 76:224–230
17. Krause-Rehberg R, Leipner HS (1999) Positron annihilation in semiconductors. Defect studies. Springer, Berlin-Heidelberg-New York
18. Jean YC, Mallon PE, Schrader DM (2003) Principles and application of positron and positronium chemistry. Word Scientific, Singapore
19. Mogensen OE (1995) Positron annihilation in chemistry. Springer, Berlin
20. Klym H, Hadzaman I, Shpotyuk O, Fu Q, Luo W, Deng J (2013) Integrated thick-film p-i-p^+ structures based on spinel ceramics. Solid State Phenom 200:156–161
21. Hadzaman I, Klym H, Shpotyuk O, Brunner M (2010) Temperature sensitive spinel-type ceramics in thick-film multilayer performance for environment sensors. Acta Phys Pol - Ser A Gen Phys 117(1):234–237
22. Klym H, Ingram A, Shpotyuk O, Calvez L, Petracovschi E, Kulyk B, Serkiz R, Szatanik R (2015) 'Cold' crystallization in nanostructurized $80GeSe_2$-$20Ga_2Se_3$ glass. Nanoscale Res Lett 10:49
23. Kansy J (1996) Microcomputer program for analysis of positron annihilation lifetime spectra. Nucl Inst Methods Phys Res A 374:235–244
24. Nambissan PMG, Upadhyay C, Verma HC (2003) Positron lifetime spectroscopic studies of nanocrystalline $ZnFe_2O_4$. J Appl Phys 93:6320
25. Tao SJ (1972) Positronium annihilation in molecular substance. J Chem Phys 56(11):5499–5510
26. Eldrup M, Lightbody D, Sherwood JN (1981) The temperature dependence of positron lifetimes in solid pivalic acid. Chem Phys 63:51–58
27. Leifer I, Patro RK (2002) The bubble mechanism for methane transport from the shallow sea bed to the surface: a review and sensitivity study. Cont Shelf Res 22(16):2409–2428
28. Ljunggren S, Eriksson JC (1997) The lifetime of a colloid-sized gas bubble in water and the cause of the hydrophobic attraction. Colloids Surf A Physicochem Eng Asp 129:151–155
29. Grosman A, Ortega C (2005) Nature of capillary condensation and evaporation processes in ordered porous materials. Langmuir 21:10515–10521
30. Dlubek G, Yang Y, Krause-Rehberg R, Beichel W, Bulut S, Pogodina N, Krossing I, Friedrich C (2010) Free volume in imidazolium triflimide ([C3MIM][NTf2]) ionic liquid from positron lifetime: amorphous, crystalline, and liquid states. J Chem Phys 133:124502